Published in final edited form as:
Retina. 2010 October ; 30(9): 1441–1454. doi:10.1097/IAE.0b013e3181ee5ce8.

Drusen Characterization with Multimodal Imaging

Richard F. Spaide, MD[*] and **Christine A. Curcio, PhD**[†]

[*] Vitreous-Retina-Macula Consultants of New York, NY LuEsther T. Mertz Retinal Research Center, Manhattan Eye, Ear & Throat Hospital, New York, NY

[†] Department of Ophthalmology, Callahan Eye Foundation Hospital, University of Alabama School of Medicine, Birmingham, AL

Abstract

Summary—Multimodal imaging findings and histological demonstration of soft drusen, cuticular drusen, and subretinal drusenoid deposits provided information used to develop a model explaining their imaging characteristics.

Purpose—To characterize the known appearance of cuticular drusen, subretinal drusenoid deposits (reticular pseudodrusen), and soft drusen as revealed by multimodal fundus imaging; to create an explanatory model that accounts for these observations.

Methods—Reported color, fluorescein angiographic, autofluorescence, and spectral domain optical coherence tomography (SD-OCT) images of patients with cuticular drusen, soft drusen, and subretinal drusenoid deposits were reviewed, as were actual images from affected eyes. Representative histological sections were examined. The geometry, location, and imaging characteristics of these lesions were evaluated. A hypothesis based on the Beer-Lambert Law of light absorption was generated to fit these observations.

Results—Cuticular drusen appear as numerous uniform round yellow-white punctate accumulations under the retinal pigment epithelium (RPE). Soft drusen are larger yellow-white dome-shaped mounds of deposit under the RPE. Subretinal drusenoid deposits are polymorphous light-grey interconnected accumulations above the RPE. Based on the model, both cuticular and soft drusen appear yellow due to the removal of shorter wavelength light by a double pass through the RPE. Subretinal drusenoid deposits, which are located on the RPE, are not subjected to short wavelength attenuation and therefore are more prominent when viewed with blue light. The location and morphology of extracellular material in relationship to the RPE, and associated changes to RPE morphology and pigmentation, appeared to be primary determinants of druse appearance in different imaging modalities.

Conclusion—Although cuticular drusen, subretinal drusenoid deposits, and soft drusen are composed of common components, they are distinguishable by multimodal imaging due to differences in location, morphology, and optical filtering effects by drusenoid material and the RPE.

Keywords

cuticular drusen; subretinal drusenoid deposits; reticular pseudodrusen; soft drusen; age-related macular degeneration

Corresponding Author: Richard F. Spaide, M.D. 460 Park Avenue, 5th Floor, New York, NY, 10022 rickspaide@yahoo.com.
The authors have no financial interests.

Introduction

Drusen are focal deposits of extracellular debris located between the basal lamina of the retinal pigment epithelium (RPE) and the inner collagenous layer of Bruch membrane found in normal aged human eyes and in eyes with age-related macular degeneration (AMD).[1–3] Drusen compositional studies over the last decade have revealed carbohydrates, zinc, and nearly 150 proteins, including vitronectin, apolipoproteins E and B, and numerous components of the complement system.[4–9] The largest single component of drusen is lipid, principally esterified cholesterol, unesterified cholesterol, and phosphatidylcholine, thought to be derived from a large lipoprotein of intra-ocular origin. [10–16]

Our appreciation of drusen is dependent on interpretations of both ocular histology and imaging. In a widely cited 1994 review,17 Bressler et al tabulated multiple histological studies of the many different entities that can masquerade as drusen-like spots in the fundus. Such potential for confusion has persisted to date, thanks in part to the explosion of new clinical imaging techniques that reveal drusen and their look-alikes in increasingly exquisite detail. 18 In addition, animal models investigated in service of understanding AMD pathobiology have added more ways that pale spots in the fundus appear similar to drusen (e.g., lipid-filled microglia or RPE cells19,20) without necessarily meeting the histological criterion. Drusen represent instructive snapshots whose size, type, and composition reveal both past formative processes16,21 and future progression of disease.[22] Thus, systematizing new knowledge from imaging and histologic studies has never been more critical, as attention turns to AMD's underlying degeneration in the wake of clinical success with VEGF inhibitors.[23]

In addition to new examination methods, the now recognized extracellular deposits themselves are more diverse, now encompassing soft drusen, cuticular drusen, and subretinal drusenoid debris. Discrete yellow-white punctate elevations ("hard" drusen) or large pale-yellow "placoid or dome-shaped structures" ("soft" drusen), seen in the fundus singly or in groups, were considered exudative drusen by Gass.24 Histopathologic investigations showed that soft drusen were mounds external to the RPE basement membrane containing membranous debris (also called "lipoprotein-derived debris"), a lipid-rich material. 16, 25–28 In contrast, multiple, densely packed small yellow-white nodular drusen that hyperfluoresce during fluorescein angiography ("starry-sky" fundus) were first termed basal laminar drusen by Gass and subsequently renamed cuticular drusenafter they were shown to contain the same constituents as soft drusen.29,30 Finally, sub-retinal drusenoid debris, originally termed "reticular pseudo-drusen",31–33 were recently identified by both histology and optic coherence tomography (OCT) as aggregations containing typical druse-associated molecules but located in the sub-retinal rather than the sub-RPE space.[26, 34, 35] Some lesions contained small zones of refractile material that could impart ophthalmoscopic features suggesting cuticular drusen.35

We hypothesized that these three different extracellular lesions with similar composition are potentially differentiable by their imaging characteristics. Here we address how contemporary imaging in fundus and cross-sectional views and based on different fundus illumination methods can be combined with histology to elucidate differences in druse appearance. We include representative clinical and histological images of different affected patients, as well as histological study of the same eyes examined clinically (indirect and direct clinicopathologic correlation, respectively). From these comparisons, we construct a model to explain the observed multimodal imaging characteristics of soft drusen, cuticular drusen, and sub-retinal drusenoid debris, based on the absorption of light by the RPE as specified by the Beer-Lambert Law.

Methods

Publications showing representative clinical and histologic cases of cuticular drusen, soft drusen, and subretinal drusenoid deposits were reviewed.[5, 6, 8, 14, 21, 24, 25, 27–46] Two recent histological cases with dry AMD were re-examined by light and transmission electron microscopy.[34] Representative clinical images used for illustrations were obtained by retrospective chart analysis. Each of these patients had undergone a complete ophthalmological examination including color photography, fundus autofluorescence (FAF), near-infrared reflectance imaging, spectral domain optical coherence tomography (SD-OCT), and fluorescein angiography. Evaluation of patient images had institutional review board approval through Western IRB and complied with the Health Insurance Portability and Accountability Act of 1996.

Near-infrared reflectance pictures were obtained with a scanning laser ophthalmoscope (SLO) that simultaneously performs spectral domain optical coherence tomography (SD-OCT) (Spectralis HRA-OCT, Heidelberg Engineering, Heidelberg, Germany). The autofluorescence images were obtained using either a confocal scanning laser ophthalmoscope (Spectralis HRA-OCT) using an excitation light of 488nm and a long-pass barrier filter starting at 500 nm or a fundus camera (Topcon Medical System, Paramus, NJ) with an excitation filter with a band pass range from 535–585 nm and a matched barrier filter with a band pass range of 605–715 nm. The SD-OCT's were obtained with the Heidelberg Spectralis (version 1.6.1) as viewed with the contained Heidelberg software (Spectralis Viewing Module 5.1.3.0; Heidelberg Engineering, Heidelberg, Germany). The Spectralis instrument allowed for topographic correlation among the SD-OCT and near-infrared images.

To examine the individual color channels of color fundus photographs, high-resolution digital color images taken with a Topcon ImageNet camera (Topcon America, Paramus, USA) were viewed either in Topcon ImageNet (version 2.55, Topcon America, Paramus NJ) or in Photoshop (Photoshop CS4, Adobe System Inc, San Jose, California). In the Topcon ImageNet program the commands Utilities>RGB channels were selected; in Photoshop the Split Channels command was used. Histogram stretching was performed on each channel independently to improve and standardize visualization of drusen. The images of each eye were analyzed to obtain comparative information concerning morphology in the color and SD-OCT images, reflectance characteristics in the blue color channel and by reflectance infrared scanning laser ophthalmoscopy and in autofluorescence images. Assembled information concerning druse visibility was used to generate a model of drusen appearance based on morphology, location, and potential induced effects on the overlying RPE.

Results

Underlying assumptions concerning imaging characteristics assembled from literature review are summarized in the text below and illustrated with the first 10 figures..

Soft drusen are yellow-white mound-like elevations typically 63 to ≥ 1000 μm in diameter. The central portion of the druse may appear slightly lighter than its edge, but druse color (Figure 1A) is not related to thickness (Figure 1D). During fluorescein angiography soft drusen are minimally hyperfluorescent in later stages, although this finding can be variable (not shown). During autofluorescence imaging the edges of some soft drusen appear slightly hyper-autofluorescent as compared with the central portion (Figure 1C), although this feature is more easily visible using a fundus camera system than it is using a scanning laser ophthalmoscopic based method of imaging.[46,47] Near infrared imaging with the SLO shows a subtle variation in the grayscale tones in regions containing drusen (Figure 1B), with a contrast much lower than that seen with conventional green light monochromatic fundus photographs. By histology

using high-resolution sections,[28] soft drusen are low mounds that can be connected by basal linear deposit (Figure 2). RPE morphology and pigmentation may be minimally affected in smaller soft drusen.[40]

Uniformly round and punctate, cuticular drusen are numerous and found in a densely packed arrangement (Figure 3). They are typically 50 to 75 μm in diameter. The definition of cuticular drusen implies a large number of adjacent drusen to achieve the starry sky appearance. The appearance of a cuticular druse in isolation may not be sufficiently distinctive to allow differentiation from other similarly sized drusen. During fluorescein angiography cuticular drusen produce multiple pinpoint sites of hyperfluorescence from the druse apices (Figure 4A), while these same locations are hypo-autofluorescent in autofluorescence imaging (Figure 3C, F). In cross-section cuticular drusen have a blunted triangular or a prolate shape (Figure 5). Cuticular drusen thus appear as a saw tooth pattern in an SD-OCT examination, where the basal diameter of each cuticular druse is about the same as its height. Limited histologic data (Figure 4B, C) indicate that cuticular drusen seem to jut into the RPE monolayer[27] such that the thickness of the overlying RPE is much less over the apex of each cuticular druse than the thickness of the RPE between drusen.

Sub-retinal drusenoid deposits show a range in size similar to that seen in soft drusen, and appear slightly blue, or at least whiter, compared with soft drusen (Figures 6, 7). Subretinal drusenoid deposits may have a more punctate appearance closer to the macular center. In addition they may appear whitish near their apex, elsewhere in the macula. The fluorescein angiographic findings of subretinal drusenoid deposits are subtle, ranging from no demonstrable change to minimal hypofluorescence.[48] In near infrared reflectance imaging with the SLO, subretinal drusenoid deposits appear darker than the uninvolved surrounding areas (Figure 6B), as they do with autofluorescence imaging (Figure 6C).[35] By OCT (Figure 6D, 7C), subretinal drusenoid deposits are seen in the subretinal space of attached retinas, above the RPE. The horizontal extent of subretinal drusenoid deposits vary with imaging method; the deposits appear somewhat smaller in infrared reflectance SLO images than they do in either color photographs or SD-OCT scans (compare Figure 6B vs 6D). They are often interconnected so that their sizes range from 25 to >1000 μm. By OCT or histology, subretinal drusenoid deposits vary in shape and thickness above the RPE, appearing as conical (Figures 6D, 8A) or flattened (Figures 7C, 9). They can be large enough to disturb or shorten the overlying photoreceptors (Figure 8A), and conical accumulations can breach the external limiting membrane.[35]

All three lesions are schematized in Figure 10. Each lesion type appears to share some similarities in composition with the others (compare subretinal debris contents in Figure 8C to soft druse contents in Figure 8D). As we develop more fully below, the vertical location of each lesion along the light path (Figure 10) contributes to the distinctive appearances in different imaging modalities.

Beer-Lambert Law and the RPE: A Model

The Beer – Lambert Law describes the proportion of light passing thorough an absorptive medium. The absorbance at any given wavelength is related to the natural log of the ratio of the incident intensity of light at that wavelength and the intensity of light passing through the medium, assuming that absorbing particles are small and do not shadow each other. The Beer-Lambert law is stated as

$$I=I_O e^{-u_a x}$$

where I is the intensity transmitted of the incident intensity I_O through a medium with an extinction coefficient u_a and a thickness x.

Melanin (eumelanin) is a brown-black polymer of dihydroxyindole carboxylic acid and its reduced forms. Within RPE, melanin is found in rod-shaped organelles predominantly in the apical cytoplasm and in the apical processes that envelop photoreceptor outer segment tips. The structural arrangement of melanosomes has the potential to violate the underlying assumptions of the derivation of the Beer-Lambert equation, however absorption coefficients have been determined for melanosomes and follow the expression[49,50]:

$$u_a = \frac{6.49 \times 10^{12}}{\lambda^{3.48}}$$

By this calculation, RPE melanosomes absorb more light with decreasing wavelength, i.e., light from the blue end of the visible spectrum.

Transmission of light through RPE is reduced in a wavelength-dependent manner, represented by the different lengths of red, green and blue arrows in Figure 11. We illustrate this concept by an analogy to sunlight and clouds (Figure 11). White light is often defined by sunlight at noon, when clouds appear white. When the sun is lower in the sky, shorter wavelengths are increasingly filtered from sunlight, due to the greater path length through blue-scattering atmosphere.[51] Figure 11 shows both white and yellow clouds just after sunrise. These clouds are different colors due to the amount of blue-filtering atmosphere that sunlight passes through, i.e., less for high white cirrus clouds, more for low yellow cumulus clouds. The composition of the clouds has not changed, but our perception of cloud color is influenced by the illuminating light. In a similar fashion the actual material in soft drusen is white, with an appearance similar to uncolored paraffin.[7] For soft drusen to be visible, light illuminating them must pass through the RPE twice, selectively reducing blue light each time so the observed color is yellow (Figure 12).

Predictions of the model

Here we characterize the spectrum of light reflecting from different lesions. Ideally, our model should include flux of the illuminating light as a function of wavelength, transmission properties of the cornea, crystalline lens and vitreous, and so forth. However in comparing one druse to another within an eye many of these features remain constant. Therefore, only the reflection term is shown below. Subretinal drusenoid deposits are located above the RPE. Light reflecting from these deposits of a given thickness would vary across the wavelengths examined by a function related to

$$\int_{\lambda=380}^{780} R_{SDD}(\lambda) d\lambda$$

where $R_{SDD}(\lambda)$ is the reflectance of light from the subretinal drusenoid deposit as a function of wavelength λ, where λ ranges from wavelengths used by SD-OCT through those visible by the eye. The material in soft drusen would have a reflectance profile of

$$\int_{\lambda=380}^{780} R_{SD}(\lambda) d\lambda$$

$R_{SD}(\lambda)$ is the reflectance of light from the soft druse material as a function of wavelength λ. Given that subretinal drusenoid deposits and soft druse have similar composition, the reflectance profiles from the actual material would probably be similar, so that $\int_{\lambda=380}^{780} R_{SDD}(\lambda)d\lambda \sim \int_{\lambda=380}^{780} R_{SD}(\lambda)d\lambda$ if the material thickness was the same. However the light returning to the observer from soft drusen would be represented by

$$\int_{\lambda=380}^{780} R_{SD}(\lambda)(T_{RPE}(\lambda))^2 d\lambda$$

because soft drusen are not directly visualized; they are under the RPE. T_{RPE} is the transmission of light by the RPE as a function of wavelength λ. This value is squared because of the double pass through the RPE.

This model allows us to make predictions about contrast between subretinal drusenoid deposits, soft drusen, and the background, and to test these predictions by separating the color channels of digital color photographs (Figure 13,14). The subject contrast (C_S) between the subretinal drusenoid deposits and the underlying layers is expressed by

$$C_S = \frac{(R_{SDD} - R_B)}{R_B}$$

in which R_{SDD} is the reflectance from the deposit and R_B is the reflection from the background, deeper layers. C_S is wavelength-dependent, as are the proportion of light absorbed, the proportion of light penetrating to deeper layers, and the amount of reflection from deeper layer components. At short wavelengths, where melanin preferentially absorbs, less light is reflected, the RPE offers a dark background, and the observed contrast of subretinal drusenoid deposits increases markedly (Figure 13D). Further, subretinal drusenoid deposits are situated in the light path in front of significant reflectors for near-infrared light, which for wavelengths used by commercial SLO, include melanin of the RPE and choroidal melanocytes as well as sclera.[52–54] At long wavelengths, then, light penetrates RPE melanin and reflects back from the choroidal blood vessels, greatly reducing the contrast between subretinal deposits and the background (Figure 13B). In contrast, the light reflecting back from soft drusen is strongly shifted towards red because blue light has been absorbed by the overlying RPE. Thus, soft drusen appear bright in the red channel (Figure 14B) and dim in the blue channel (Figure 14D) of a color photograph, unlike subretinal drusenoid debris in the same eye.

Our model also potentially explains the appearance of cuticular drusen, which are small and resemble vertically oriented ellipses in cross-section. Attenuation of the overlying RPE would position fewer fluorophores in the optical path for autofluorescence imaging and decrease the amount of pigment blocking the excitation light for fluorescein angiography. This would produce decreased central autofluorescence with concomitant hyperfluorescence in fluorescein angiography (Figure 6C). The variable attenuation of light also causes observable changes in the SD-OCT characteristics of these drusen (Figure 15). The RPE appears to be thicker around the base of each cuticular drusen than at its apex. The thickened RPE causes shadowing and increased light penetration into deeper layers from the apex of each individual druse (Figure 15).

Discussion

Although the composition of soft drusen, cuticular drusen, and subretinal drusenoid deposits share similarities, they are differentiable by multimodal imaging when the RPE's position and light absorption characteristics are taken into account. These distinctions are important to make, because refined interpretation of these lesions will ultimately permit more accurate risk assessment for disease progression. Our observations are possible now due to newer instrumentation that provides both sufficiently high resolution and multiple modalities within single devices.

In addition to lesion composition, size, and shape, key determinants of lesion appearance are position of extracellular material with respect to the RPE and changes in RPE morphology and pigmentation affecting light filtering by these cells. Both soft drusen and cuticular drusen are subject to variable amount of blue light attenuation due to their location under the RPE. The appearance of typical sub-RPE drusen is therefore a function of not only the reflectance characteristics of the lesion itself but also RPE-associated optical filtering. The relative sizes of cuticular and soft drusen further affect their appearances. Due to the large size of soft drusen, the attenuation in thickness of the overlying RPE from center to edge is gradual. Relative to soft drusen, cuticular drusen are much smaller. RPE thickness changes more abruptly, and local differences in radial thicknesses therefore are much more extreme. The distinctive shape of RPE overlying cuticular drusen affects both the fluorescein angiogram and autofluorescence from these lesions. Variation in RPE thickness is thought to explain the observation that soft drusen have slightly hyperautofluorescent edges and slightly hypoautofluorescent centers.[46] A similar, but more exaggerated effect would apply to cuticular drusen, positioning fewer melanosomes and lysosomes over the druse center and proportionately more over the outer boundaries. Decreased fluorophores in the light path would lead to decreased autofluorescence, and decreased melanin in the light path would allow greater passage of both the excitation and emission wavelengths for fluorescein angiography. In contrast, subretinal drusenoid deposits are internal to the RPE, and consequently light striking them is not filtered by the RPE.

Our observations concerning subretinal drusenoid deposits illustrate the concept that all modes of imaging available to us were necessary to interpret these lesions definitively. Subretinal drusenoid deposits are associated with a reticular pattern of decreased autofluorescence. SD-OCT and histopathologic examination has shown that subretinal drusenoid deposits, originally called reticular pseudodrusen, are actually located in the subretinal space and are not explained by post-mortem retinal detachment. Because of the material's position in the optical path, its reflectance, absorption, and scattering of light would affect the amount of light reaching deeper layers such as the RPE and additionally the return of light from those layers. Alternate explanations for the appearance of these lesions in the fundus have been recently proposed. A recent study hypothesized that reticular pseudodrusen involved multiple layers and sought to visualize tissue damage in each layer in turn by different acquisition methods. Since different methods implicated either the RPE, choriocapillaris, or inner choroid, the authors concluded that all layers were involved. This "unified description" did not include the important cross-sectional perspective offered by OCT[55] and thus could not consider the possibility that reduced visualization of one layer may be subsequent to changes in an overlying layer. Without knowledge that reticular pseudodrusen are accumulations of material in the subretinal space, decreased autofluorescence observed in their presence could be attributed solely to an RPE abnormality and not to screening by the lesion.[55] Because subretinal drusenoid deposits may form a nearly confluent layer, they may be difficult to see by autofluorescence or near-infrared imaging, except at their borders where the contrast between them and the background is greater. SD-OCT thus appears to be the most reliable method of detecting both the conical and flattened forms of deposition, since this modality provides an actual demonstration of the material, as opposed to variation in grayscale levels. However there appears to be variation in the image

quality of the various commercial SD-OCT instruments and the imaging characteristics of these drusen were done with an instrument capable of image averaging to improve the signal to noise ratio.

The current study attempts to explain known patterns observed with several druse types, each sharing similarities in composition. As such this study functions to organize available information, which is likely to be incomplete. A paucity of histopathologic information about eyes previously imaged in the clinic is a shortcoming of most ocular imaging studies, including this one. However integrating information from different imaging modes yielded an internally consistent hypothesis that appears to explain many aspects of druse appearance. This model potentially explains, in general terms, the spectral profile of reflected light from various drusen types, expected angiographic findings, and autofluorescence imaging results. Further research may provide more quantitative means to differentiate drusen based on multimodal imaging. Further, histological studies may provide quantitative measures of the cells, layers, and extracellular materials imaged by these methods.

Acknowledgments

This work is supported in part by The Macula Foundation, Inc. CAC is supported by an NIH grant EY06109, the EyeSight Foundation of Alabama, International Retinal Research Foundation, The Thome Foundation, and unrestricted funds to the Department of Ophthalmology from Research to Prevent Blindness Inc.

References

1. Bressler, SB.; Bressler, NM.; Sarks, SH.; Sarks, JP. Age-related macular degeneration: nonneovascular early AMD, intermediate AMD, and geographic atrophy. In: Ryan, SJ., editor. Retina. Mosby; 2006. p. 1041-1074.
2. Klein R, Klein BEK, Linton KLP. Prevalence of age-related maculopathy. Ophthalmol 1992;99:933–943.
3. van der Schaft TL, Mooy CM, de Bruijn WC, et al. Histologic features of the early stages of age-related macular degeneration. Ophthalmol 1992;99:278–286.
4. Mullins RF, Hageman GS. Human ocular drusen possess novel core domains with a distinct carbohydrate composition. J Histochem Cytochem 1999;47:1533–1539. [PubMed: 10567437]
5. Mullins RF, Russell SR, Anderson DH, Hageman GS. Drusen associated with aging and age-related macular degeneration contain proteins common to extracellular deposits associated with atherosclerosis, elastosis, amyloidosis, and dense deposit disease. FASEB J 2000;14:835–846. [PubMed: 10783137]
6. Anderson DH, Ozaki S, Nealon M, et al. Local cellular sources of apolipoprotein E in the human retina and retinal pigmented epithelium: implications for the process of drusen formation. Am J Ophthalmol 2001;131:767–781. [PubMed: 11384575]
7. Crabb JW, Miyagi M, Gu X, et al. Drusen proteome analysis: an approach to the etiology of age-related macular degeneration. Proc Natl Acad Sci U S A 2002;99:14682–7. [PubMed: 12391305]
8. Malek G, Li C-M, Guidry C, et al. Apolipoprotein B in cholesterol-containing drusen and basal deposits in eyes with age-related maculopathy. Am J Pathol 2003;162:413–425. [PubMed: 12547700]
9. Lengyel I, Flinn JM, Peto T, et al. High concentration of zinc in sub-retinal pigment epithelial deposits. Exp Eye Res 2007;84:772–80. [PubMed: 17313944]
10. Wolter JR, Falls HF. Bilateral confluent drusen. Arch Ophthalmol 1962;68:219–226. [PubMed: 14008122]
11. Pauleikhoff D, Zuels S, Sheraidah GS, et al. Correlation between biochemical composition and fluorescein binding of deposits in Bruch's membrane. Ophthalmol 1992;99:1548–1553.
12. Curcio CA, Millican CL, Bailey T, Kruth HS. Accumulation of cholesterol with age in human Bruch's membrane. Invest Ophthalmol Vis Sci 2001;42:265–274. [PubMed: 11133878]

13. Haimovici R, Gantz DL, Rumelt S, et al. The lipid composition of drusen, Bruch's membrane, and sclera by hot stage polarizing microscopy. Invest Ophthalmol Vis Sci 2001;42:1592–1599. [PubMed: 11381066]
14. Curcio CA, Presley JB, Medeiros NE, et al. Esterified and unesterified cholesterol in drusen and basal deposits of eyes with age-related maculopathy. Exp Eye Res 2005;81(6):731–741. [PubMed: 16005869]
15. Wang L, Clark ME, Crossman DK, et al. Abundant lipid and protein components of drusen. PLoS ONE 2010;5:e10329. [PubMed: 20428236]
16. Curcio CA, Johnson M, Huang J-D, Rudolf M. Aging, age-related macular degeneration, and the Response-to-Retention of apolipoprotein B-containing lipoproteins. Prog Ret Eye Res 2009;28:393–422.
17. Bressler NM, Silva JC, Bressler SB, et al. Clinicopathological correlation of drusen and retinal pigment epithelial abnormalities in age-related macular degeneration. Retina 1994;14:130–142. [PubMed: 8036323]
18. Khanifar AA, Koreishi AF, Izatt JA, Toth CA. Drusen ultrastructure imaging with spectral domain optical coherence tomography in age-related macular degeneration. Ophthalmology 2008;115:1883–90. [PubMed: 18722666]
19. Raoul W, Feumi C, Keller N, et al. Lipid-bloated subretinal microglial cells are at the origin of drusen appearance in CX3CR1-deficient mice. Ophthalmic Res 2008;40:115–9. [PubMed: 18421223]
20. Anderson MD, Dawson WW, Martinez-Gonzalez J, Curcio CA. Drusenoid lesions and lipid-filled retinal pigment epithelium cells in a rhesus macula. Vet Ophthalmol 2006;9:201–207. [PubMed: 16634936]
21. Hageman GS, Luthert PJ, Chong NHC, et al. An integrated hypothesis that considers drusen as biomarkers of immune-mediated processes at the RPE-Bruch's membrane interface in aging and age-related macular degeneration. Progr Ret Eye Res 2001;20:705–732.
22. Klein R, Klein BE, Knudtson MD, et al. Fifteen-year cumulative incidence of age-related macular degeneration: the Beaver Dam Eye Study. Ophthalmology 2007;114:253–62. [PubMed: 17270675]
23. Rosenfeld PJ, Brown DM, Heier JS, et al. Ranibizumab for neovascular age-related macular degeneration. N Engl J Med 2006;355:1419–31. [PubMed: 17021318]
24. Gass, JDM. Stereoscopic atlas of macular diseases: diagnosis and treatment. 4. St. Louis: Mosby; 1997.
25. Green WR, Enger C. Age-related macular degeneration histopathologic studies: the 1992 Lorenz E. Zimmerman Lecture Ophthalmology 1993;100:1519–1535.
26. Sarks JP, Sarks SH, Killingsworth MC. Evolution of geographic atrophy of the retinal pigment epithelium. Eye 1988;2:552–577. [PubMed: 2476333]
27. Sarks JP, Sarks SH, Killingsworth MC. Evolution of soft drusen in age-related macular degeneration. Eye 1994;8:269–283. [PubMed: 7525362]
28. Curcio CA, Millican CL. Basal linear deposit and large drusen are specific for early age-related maculopathy. Arch Ophthalmol 1999;117:329–339. [PubMed: 10088810]
29. Russell SR, Mullins RF, Schneider BL, Hageman GS. Location, substructure, and composition of basal laminar drusen compared with drusen associated with aging and age-related macular degeneration. Am J Ophthalmol 2000;129:205–14. [PubMed: 10682974]
30. Leng T, Rosenfeld PJ, Gregori G, et al. Spectral domain optical coherence tomography characteristics of cuticular drusen. Retina 2009;29:988–93. [PubMed: 19584657]
31. Mimoun G, Soubrane G, Coscas G. Macular drusen. J Fr Ophtalmol 1990;13:511–30. [PubMed: 2081842]
32. Arnold JJ, Sarks SH, Killingsworth MC, Sarks JP. Reticular pseudodrusen. A risk factor in age-related maculopathy. Retina 1995;15:183–191. [PubMed: 7569344]
33. Cohen SY, Dubois L, Tadayoni R, et al. Prevalence of reticular pseudodrusen in age-related macular degeneration with newly diagnosed choroidal neovascularisation. Br J Ophthalmol 2007;91:354–9. [PubMed: 16973663]
34. Rudolf M, Malek G, Messinger JD, et al. Sub-retinal drusenoid deposits in human retina: organization and composition. Exp Eye Res 2008;87:402–408. [PubMed: 18721807]

35. Zweifel SA, Spaide RF, Curcio CA, et al. Reticular pseudodrusen are subretinal drusenoid deposits. Ophthalmology 2010;117:303–12.e.1. [PubMed: 19815280]
36. Gass JD, Jallow S, Davis B. Adult vitelliform macular detachment occurring in patients with basal laminar drusen. Am J Ophthalmol 1985;99:445–59. [PubMed: 3985082]
37. Sarks SH, Arnold JJ, Killingsworth MC, Sarks JP. Early drusen formation in the normal and aging eye and their relation to age-related maculopathy: a clinicopathological study. Br J Ophthalmol 1999;83:358–368. [PubMed: 10365048]
38. Sarks S, Cherepanoff S, Killingsworth M, Sarks J. Relationship of basal laminar deposit and membranous debris to the clinical presentation of early age-related macular degeneration. Invest Ophthalmol Vis Sci 2007;48:968–77. [PubMed: 17325134]
39. Li C-M, Clark M, Rudolf M, Curcio CA. Distribution and composition of esterified and unesterified cholesterol in extra-macular drusen. Exp Eye Res 2007;85:192–201. [PubMed: 17553492]
40. Rudolf M, Clark ME, Chimento M, et al. Prevalence and morphology of druse types in the macula and periphery of eyes with age-related maculopathy. Invest Ophthalmol Vis Sci 2008;49:1200–1209. [PubMed: 18326750]
41. Spraul CW, Grossniklaus HE. Characteristics of drusen and Bruch's membrane in postmortem eyes with age-related macular degeneration. Arch Ophthalmol 1997;115:267–273. [PubMed: 9046265]
42. van der Schaft TL, de Bruijn WC, Mooy CM, et al. Element analysis of the early stages of age-related macular degeneration. Arch Ophthalmol 1992;110:389–394. [PubMed: 1543459]
43. Hageman GS, Mullins RG, Russell SR, et al. Vitronectin is a constituent of ocular drusen and the vitronectin gene is expressed in human retinal pigmented epithelial cells. FASEB J 1999;13:477–484. [PubMed: 10064614]
44. Hageman GS, Mullins RF. Molecular composition of drusen as related to substructural phenotype. Mol Vis 1999;5:28. [PubMed: 10562652]
45. Zweifel SA, Imamura Y, Spaide TC, Fujiwara T, Spaide RF. Prevalence and significance of subretinal drusenoid deposits (reticular pseudodrusen) in age-related macular degeneration. Ophthalmology 2010;117:1775–1781. [PubMed: 20472293]
46. Delori FC, Fleckner MR, Goger DG, et al. Autofluorescence distribution associated with drusen in age-related macular degeneration. Invest Ophthalmol Vis Sci 2000;41:496–504. [PubMed: 10670481]
47. Spaide, RF. Autofluorescence imaging with the fundus camera. In: Holz, FG.; Schmitz-Valkenberg, S.; Spaide, RF.; Bird, AC., editors. Atlas of Fundus Autofluorescence Imaging. Berlin: Springer; 2007. p. 49-54.
48. Prenner JL, Rosenblatt BJ, Tolentino MJ, et al. Risk factors for choroidal neovascularization and vision loss in the fellow eye study of CNVPT. Retina 2003;23:307–14. [PubMed: 12824829]
49. Jacques, SL.; Glickman, RD.; Schwartz, JA. In: Jacques, SL., editor. Internal absorption coefficient and threshold for pulsed laser disruption of melanosomes isolated from retinal pigment epithelium; SPIE Proceedings of Laser-Tissue Interaction VII; 1996. p. 468-477.
50. Jacques SL, McAuliffe DJ. The melanosome: threshold temperature for explosive vaporization and internal absorption coefficient during pulsed laser irradiation. Photochem Photobiol 1991;53:769–75. [PubMed: 1886936]
51. Berry, R.; Burnell, J. The Handbook of Astronomical Image Processing. Richmond: Willmann-Bell; 2000.
52. Delori FC, Pflibsen KP. Spectral reflectance of the human ocular fundus. Appl Opt 1989;28:1061–1077. [PubMed: 20548621]
53. Preece SJ, Claridge E. Monte Carlo modelling of the spectral reflectance of the human eye. Phys Med Biol 2002;47:2863–77. [PubMed: 12222851]
54. Berendschot TT, DeLint PJ, van Norren D. Fundus reflectance--historical and present ideas. Prog Retin Eye Res 2003;22:171–200. [PubMed: 12604057]
55. Smith RT, Sohrab MA, Busuioc M, Barile G. Reticular macular disease. Am J Ophthalmol 2009;148:733–743e2. [PubMed: 19878758]

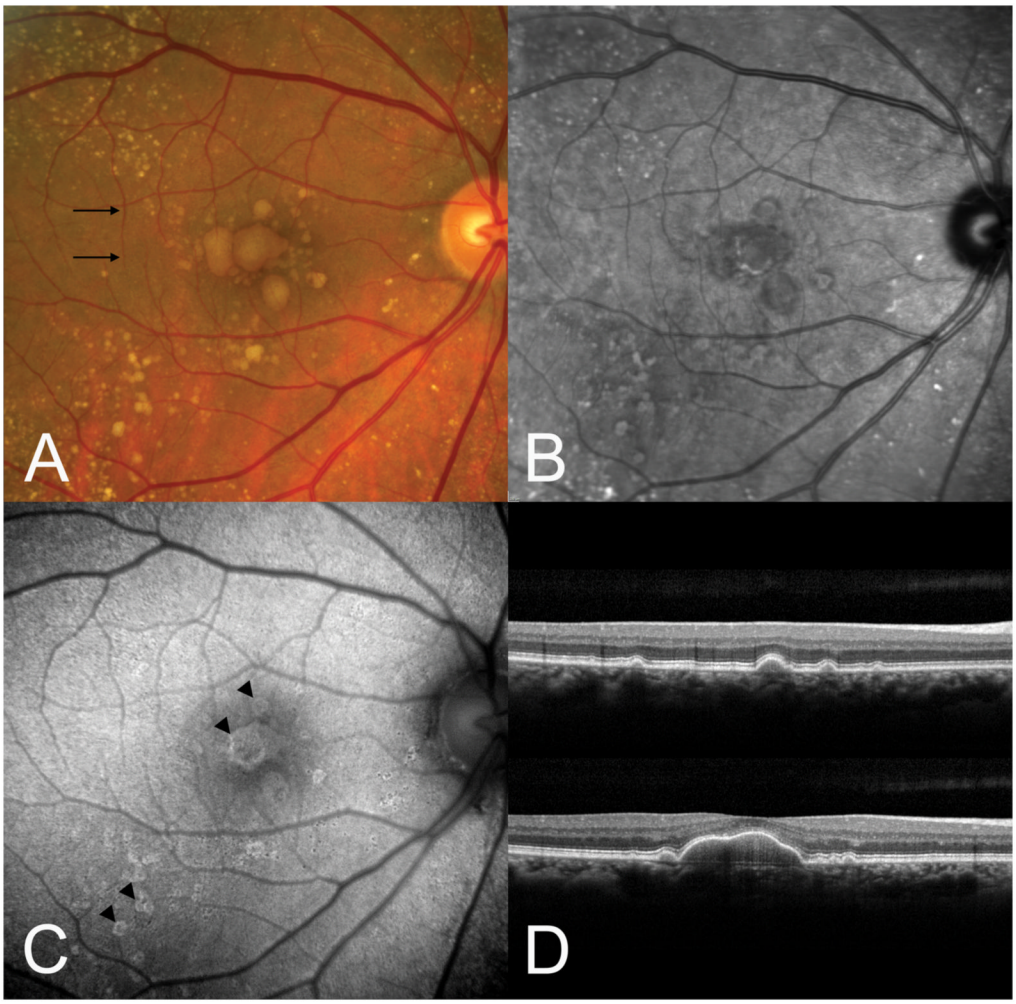

Figure 1.
Large soft drusen. A. Color photograph. The black arrows indicate the scan lines for the optical coherence tomographic (OCT) sections. B. The near-infrared reflectance scanning laser ophthalmoscopic (SLO) picture shows decreased brightness in the region of the soft drusen. C. There is a subtle increase in autofluorescence at the outer edges of several drusen. D. Representative OCT scans showing the deposition of material under the retinal pigment epithelium (RPE). Note that drusen color in A is not related to the thickness of sub-RPE material seen in D.

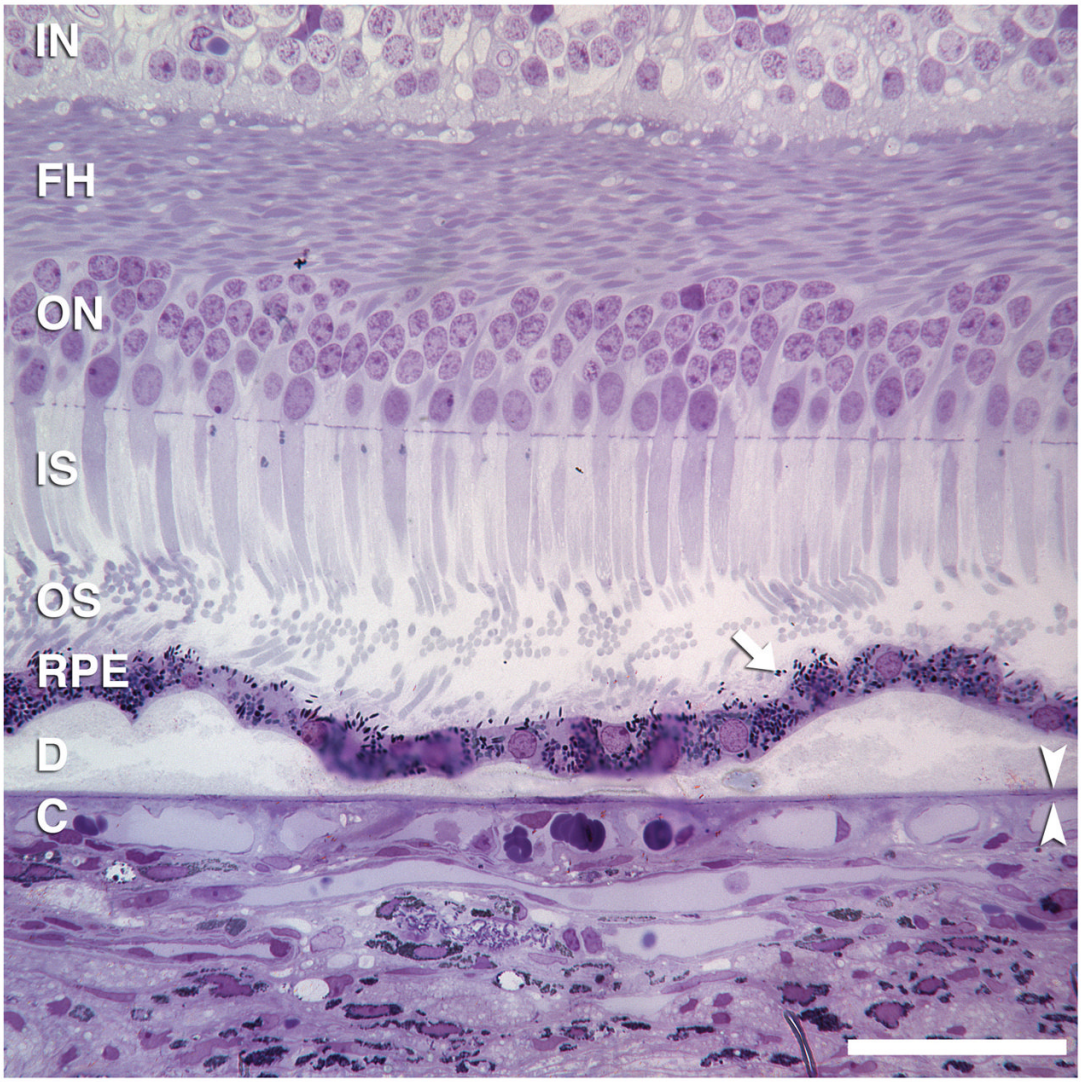

Figure 2.

Two small soft drusen connected by basal linear deposit. Drusen contain membranous debris (lipoprotein-derived debris) and neutral lipid pools. RPE morphology and pigmentation is minimally affected. Basal linear deposit has also been called diffuse drusen. 1-μm thick, toluidine-blue stained section of eye post-fixed in osmium. Scale bar, 50 μm. Retinal layers: IN, inner nuclear; FH, Fibers of Henle in the outer plexiform layer; ON, outer nuclear; IS, inner segments; OS, outer segments; RPE, retinal pigment epithelium; C, choriocapillaris. Arrow indicates individual melanin granules in RPE apical processes. Arrowheads bracket Bruch's membrane.

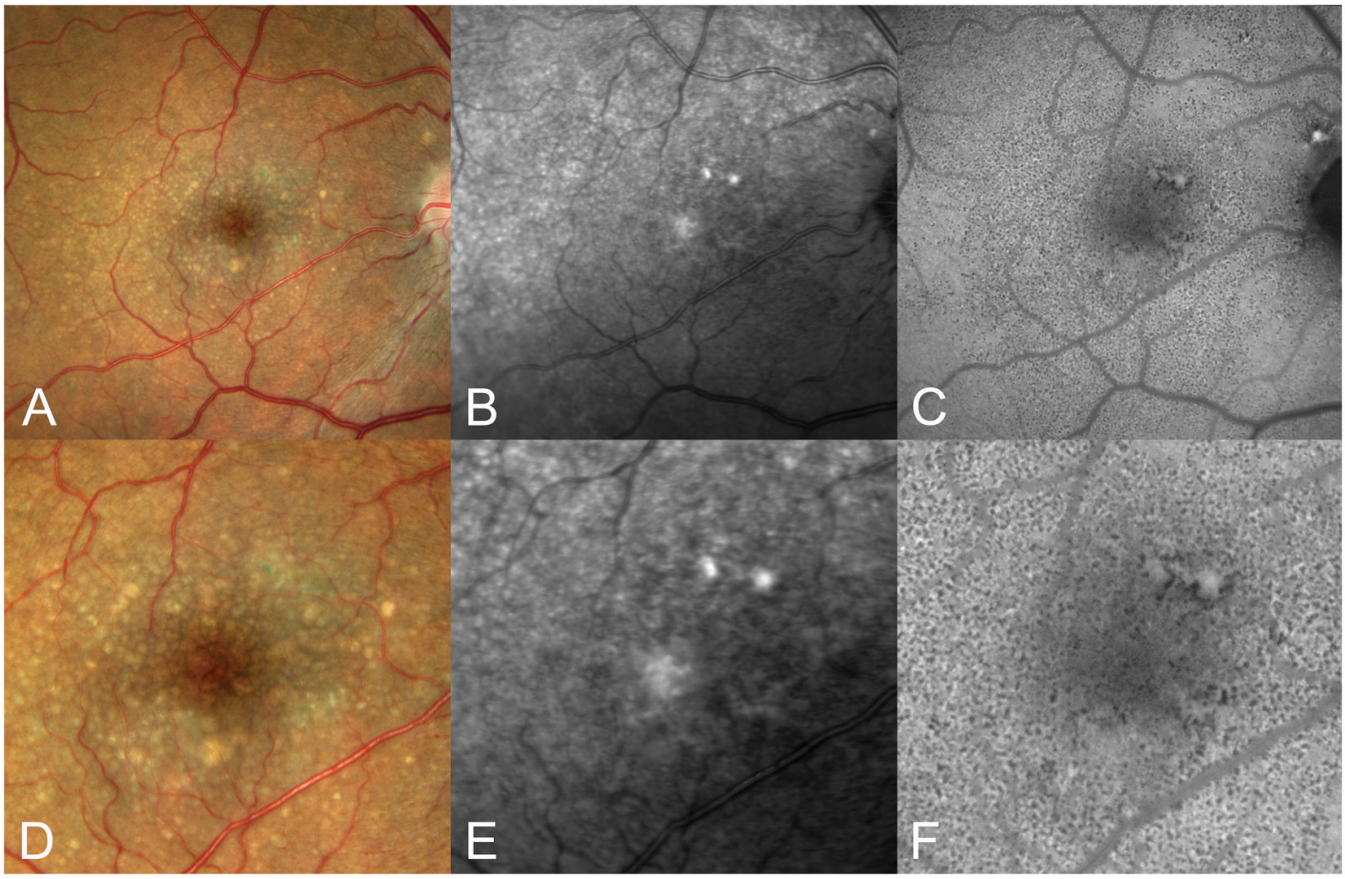

Figure 3.
Cuticular drusen. A. Color photograph; B, near-infrared SLO image, C, autofluorescence image. D-F show 200% magnifications of the central portion of A–C, respectively. Note that the numerous small drusen in the color photograph are much more difficult to see in the near infrared images. The autofluorescence image shows innumerable small hypo-autofluorescent dots. These may represent the numerical summation of both thinning of the overlying RPE and focal areas of RPE degeneration.[29]

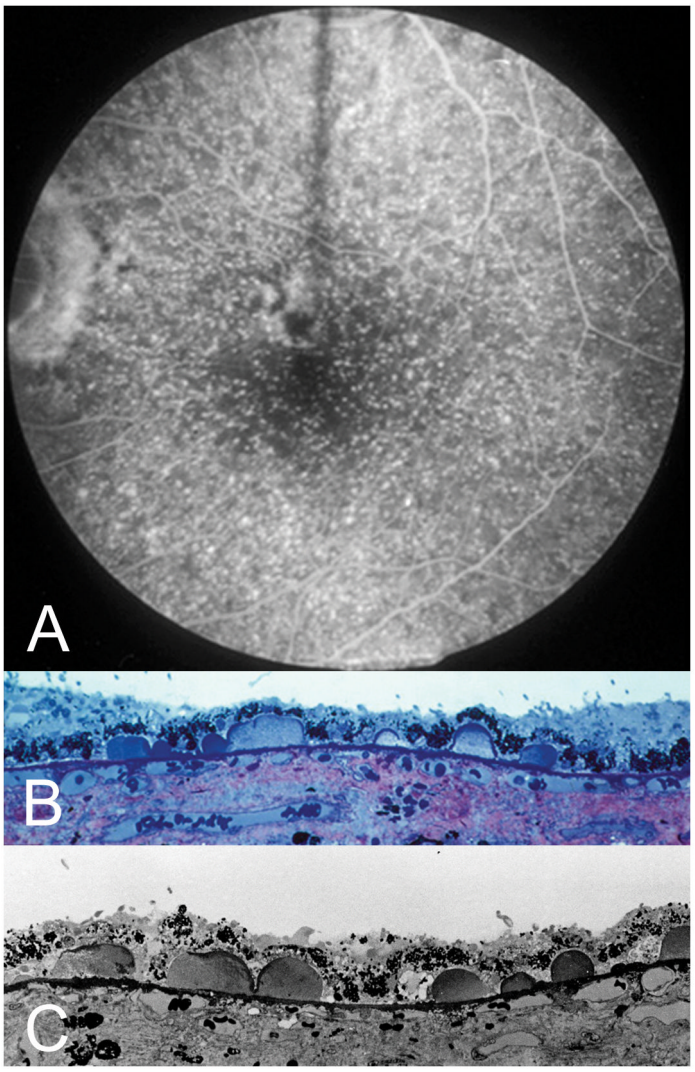

Figure 4.
Cuticular drusen, clinical and histologic images. A. Fluorescein angiography shows a starry-sky pattern of many punctate dots of hyperfluorescence. Light microscopic (B) and electron microscopic (C) of this patient at post-mortem shows numerous small ovoid accumulations protruding into the RPE monolayer. Note the thinning of the RPE over the apex, and the thickening of RPE at the base, of each druse. (Courtesy of John Sarks, MD.)

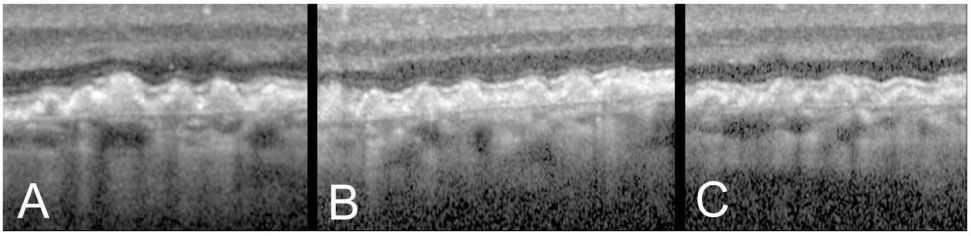

Figure 5.
OCT findings of cuticular drusen. A, B, C. OCT images from 3 different patients show closely packed blunted triangles, the bases of which sit on Bruch's membrane with apices towards the retina.

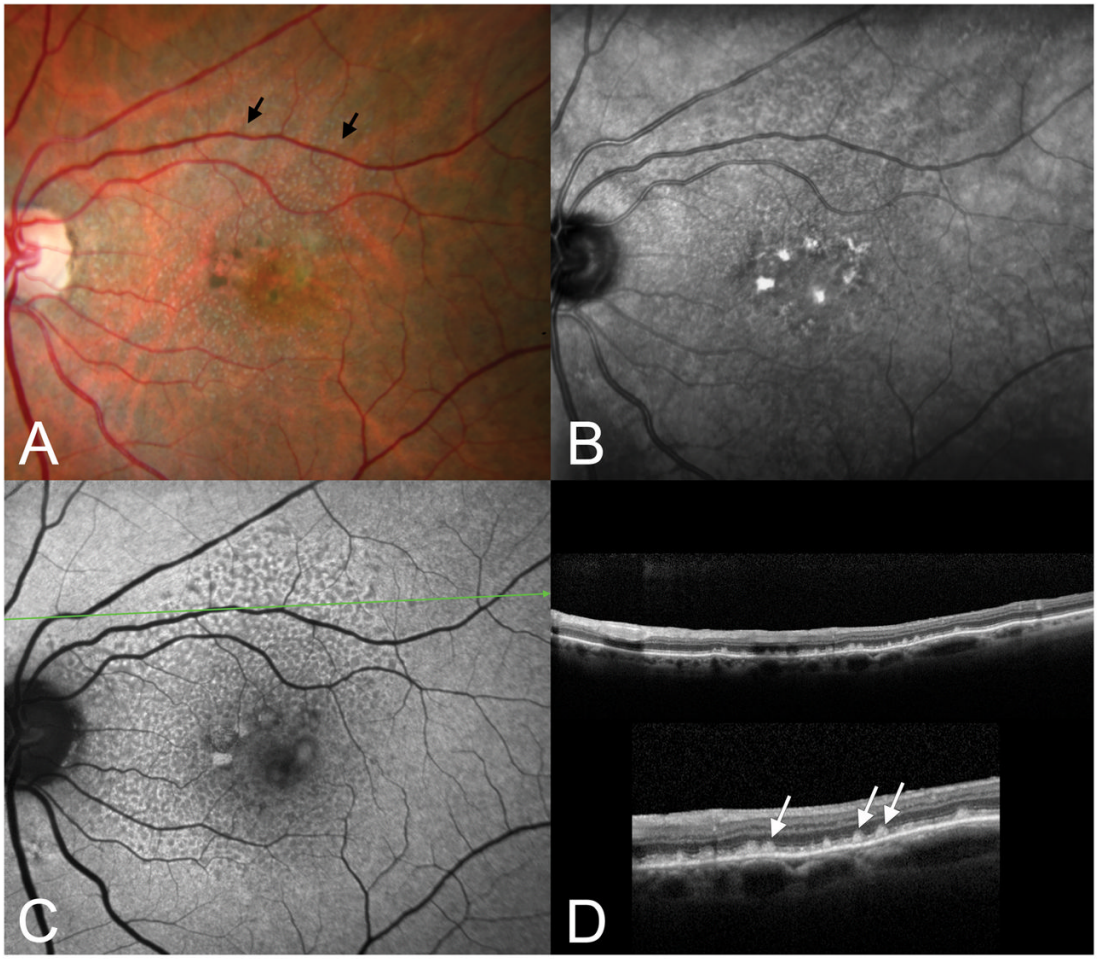

Figure 6.
Subretinal drusenoid deposits, conical. A. The color photograph shows numerous pinpoint drusen-like structures (arrows) that superficially resemble cuticular drusen. B. The near-infrared SLO image shows dark spots corresponding to the small drusenoid deposits seen in A. C. The autofluorescence image shows hypo-autofluorescent spots corresponding to the drusenoid deposits, which are seen in cross-section in the OCT (D, top). The inset in lower D shows a 200% enlargement. Note the numerous conical deposits above the RPE.

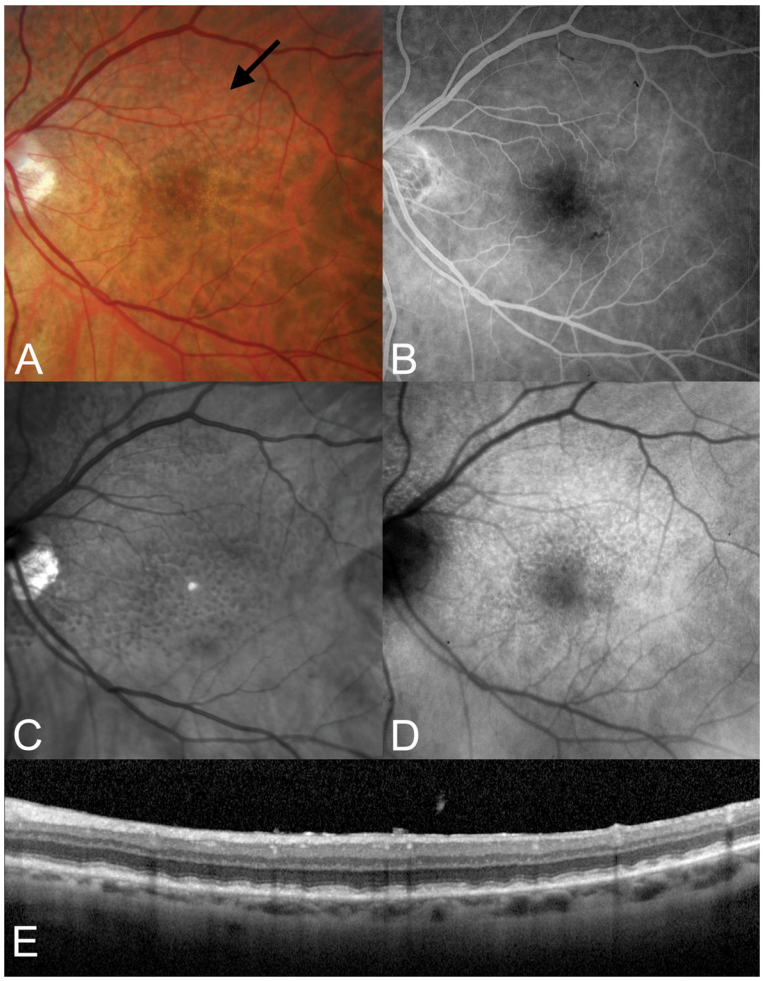

Figure 7.
Subretinal drusenoid deposits, flat. A. Subtle subretinal drusenoid deposits are visible as grayish spots in the superior macula. B. There are no corresponding findings in the fluorescein angiogram. C. The SD-OCT section shows relatively flat aggregates between the boundary between the inner and outer segments and the underlying RPE.

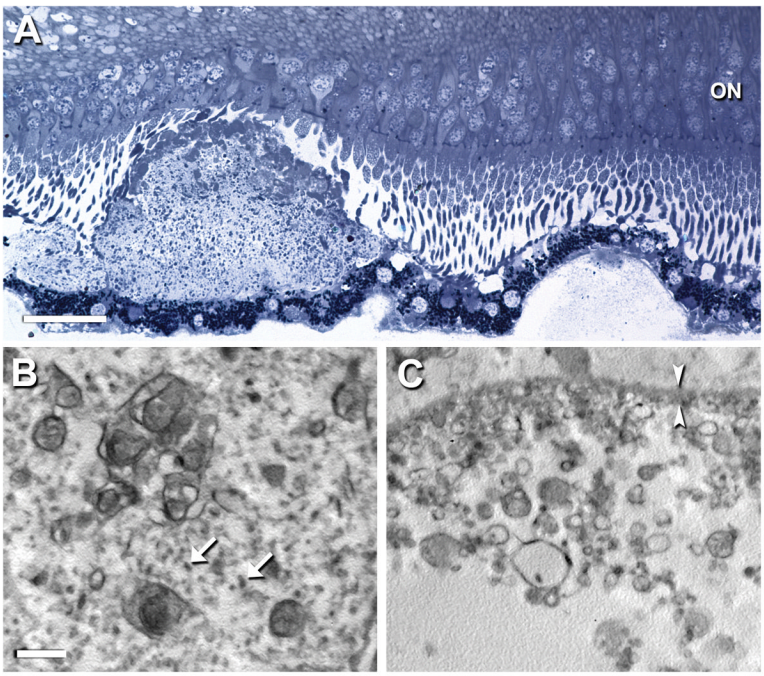

Figure 8.

Disposition and ultrastructure of subretinal drusenoid debris and soft drusen. New sections from Case 134 were post-fixed by the osmium-tannic acid-paraphenylenediamine method for neutral lipid and sectioned at 1 μm for staining with toluidine blue (A) or sectioned for transmission electron microscopy (B, C). A. Adjacent sub-retinal drusenoid deposit (at left) and soft druse (at right) that is attached to the RPE. The subretinal drusenoid deposit is well-formed, with overlying photoreceptors that are deflected or shortened. It includes an apical cap of material, distinct from outer segments in both staining density and size, and possibly corresponding to an acetone-resistant cap previously described.35 The soft druse has partial contents that bind little stain. Both RPE underlying the deposit and overlying the druse is minimally disturbed. Bar, 25 μm. ON, outer nuclear layer. B, C. The interior of the subretinal drusenoid deposit has complex membranous whorls with neutral lipid interiors dispersed throughout a ground substance with globular proteins (arrows). In contrast, the soft druse has membranous debris of simpler shapes, mostly spheres, and heterogeneous sizes. Much of the druse contents are missing, consistent with the known physical fragility of these lesions [40]. Globular proteins present in B are absent in C. Other ultrastructural descriptions using osmium post-fixation indicate that subretinal drusenoid debris and soft drusen both contain abundant membranous debris [26]. Bar, 1 μm. Bracketing arrowheads indicate RPE basal lamina. (Prepared by Jeffrey D. Messinger, DC).

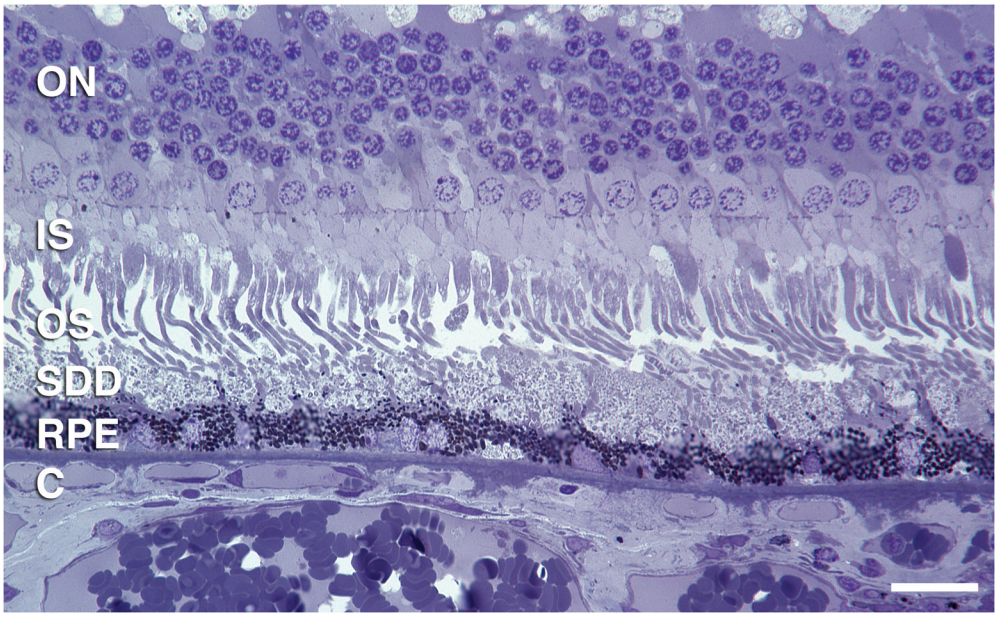

Figure 9.
Flattened subretinal drusenoid debris. Histological section was prepared as described in Figure 8A. Layers are labeled as in Figure 2. Bar, 20 μm.

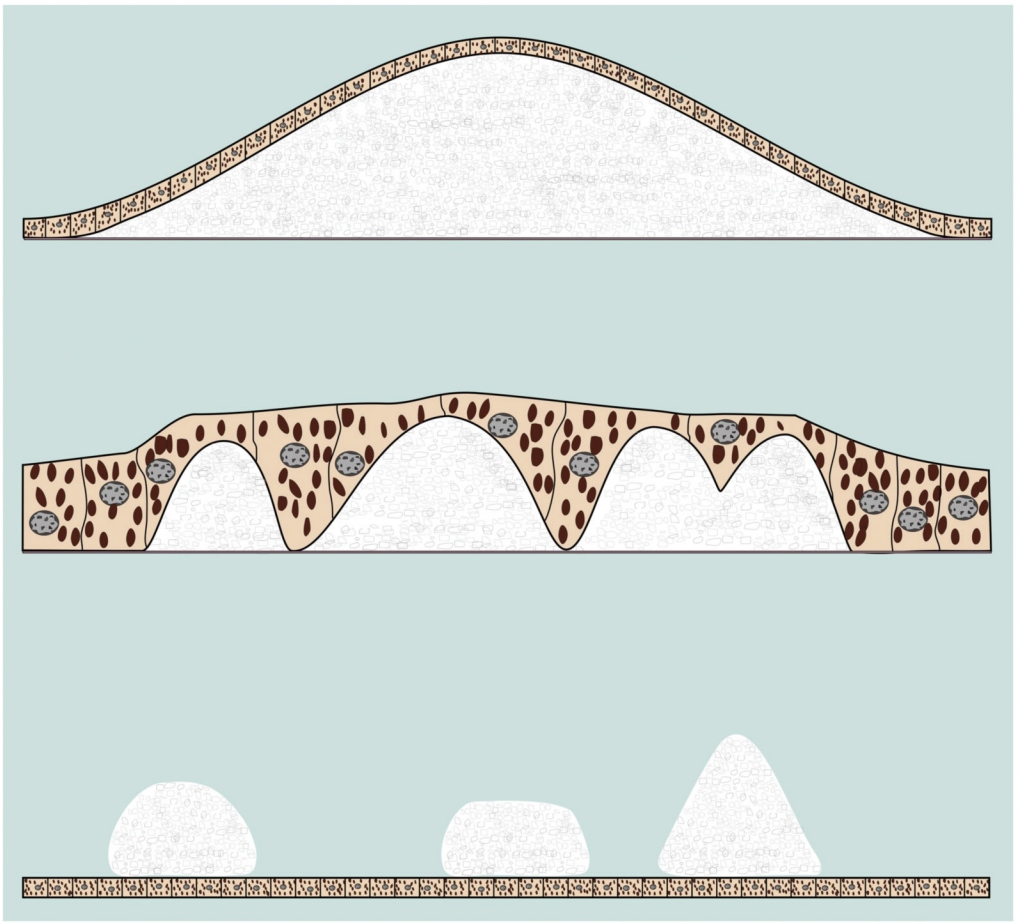

Figure 10.
Schematic of lesion sizes, shapes, and relations with RPE. Soft drusen are formed by mounds of deposit under the RPE. Soft drusen generally range in size from 63 to greater than 1000 microns in diameter. There may be some attenuation of the RPE over the apex of the druse. Cuticular drusen are 50 to 75 microns in diameter and jut up through the thickness of the overlying RPE. Subretinal drusenoid deposits show a range of sizes larger than that of soft drusen; they can be confluent and consequently be quite large but also can have refractile elements that emulate the appearance of cuticular drusen.[35]

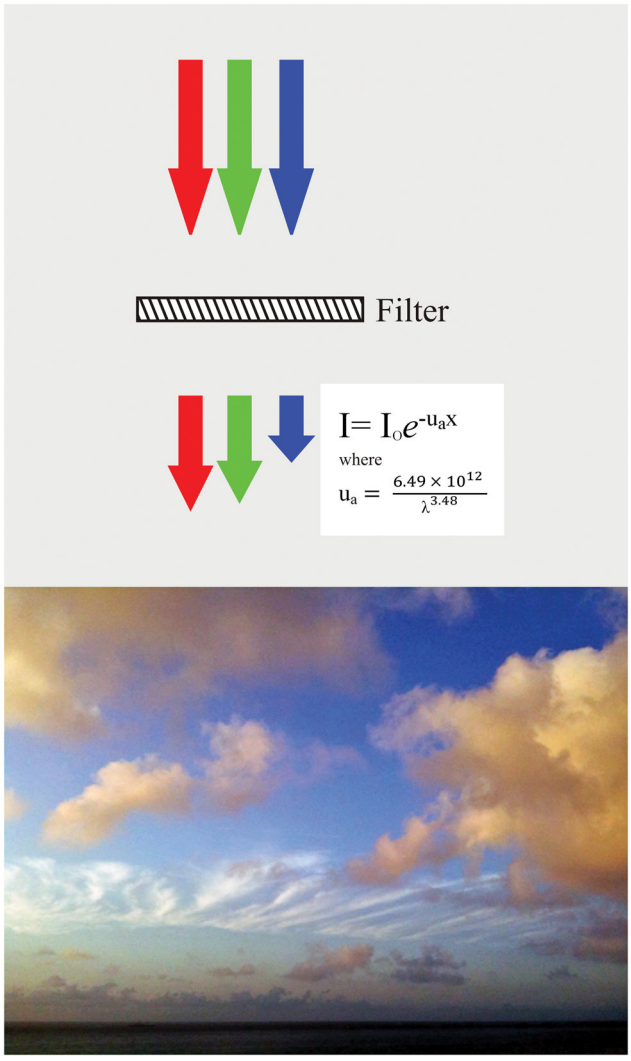

Figure 11.

Spectral filtering of light by RPE and atmosphere. Left, The RPE attenuates light, particularly for shorter wavelengths of light as shown by the varying nature of the extinction coefficient u_a. If white light, illustrated as red, green, and blue arrows of equivalent lengths to represent equivalent intensities, pass through a filter with the optical qualities of the RPE, the blue light is preferentially absorbed. The resultant spectral profile is similar to that of sunlight. Right, When the sun is low in the sky, shorter wavelengths are increasingly filtered from sunlight, due to the greater path length through blue-scattering atmosphere. Clouds are therefore different colors due to the amount of blue-filtering atmosphere that sunlight passes through, i.e., less for high white cirrus clouds, more for low yellow cumulus clouds. By analogy, the material in soft drusen appears yellow by ophthalmoscopy not because druse contents are yellow, but because of optical filtering by the overlying RPE.

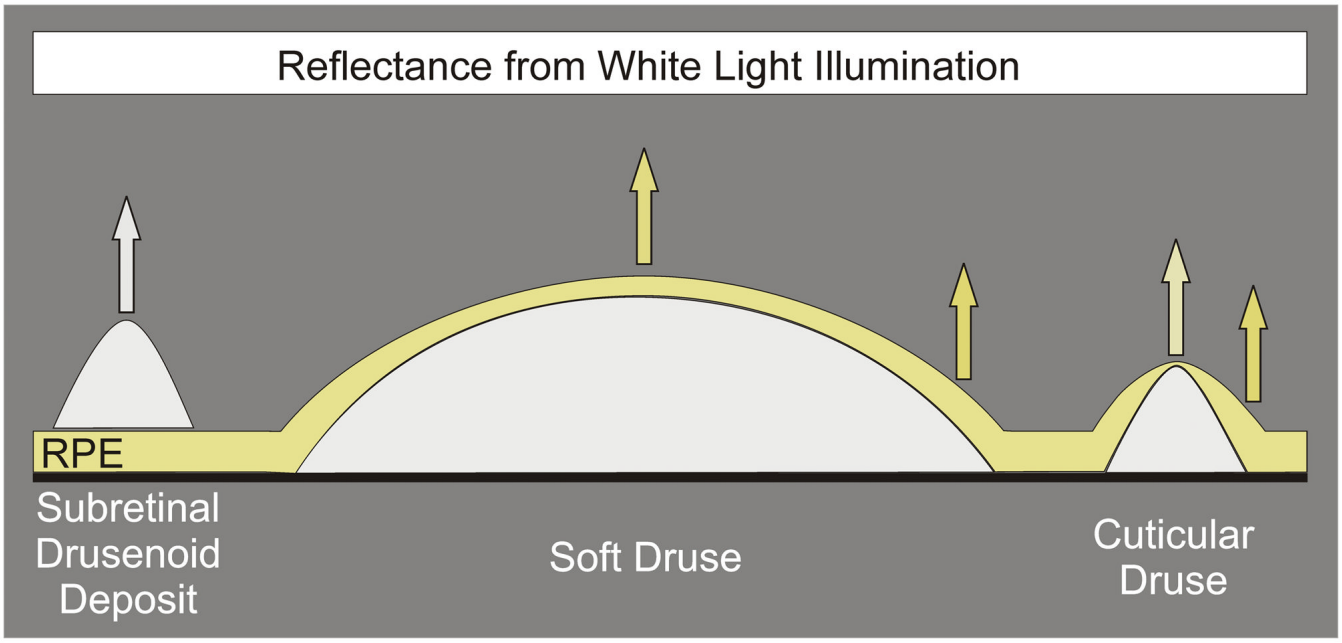

Figure 12.
The RPE absorbs and attenuates blue light. Subretinal drusen deposits are on top of the RPE and therefore do not have any blue light attenuation. Soft and cuticular drusen, in contrast, are under the RPE, which attenuates blue light in their reflective spectral profiles. Local thickness changes in the overlying RPE are more acute for cuticular drusen than for soft drusen. RPE thickness at the apex of a cuticular druse is less than at the druse edge. This positions less pigment to block the excitation light used in fluorescein angiography and may account for the pinpoint hyperfluorescence seen with these drusen.

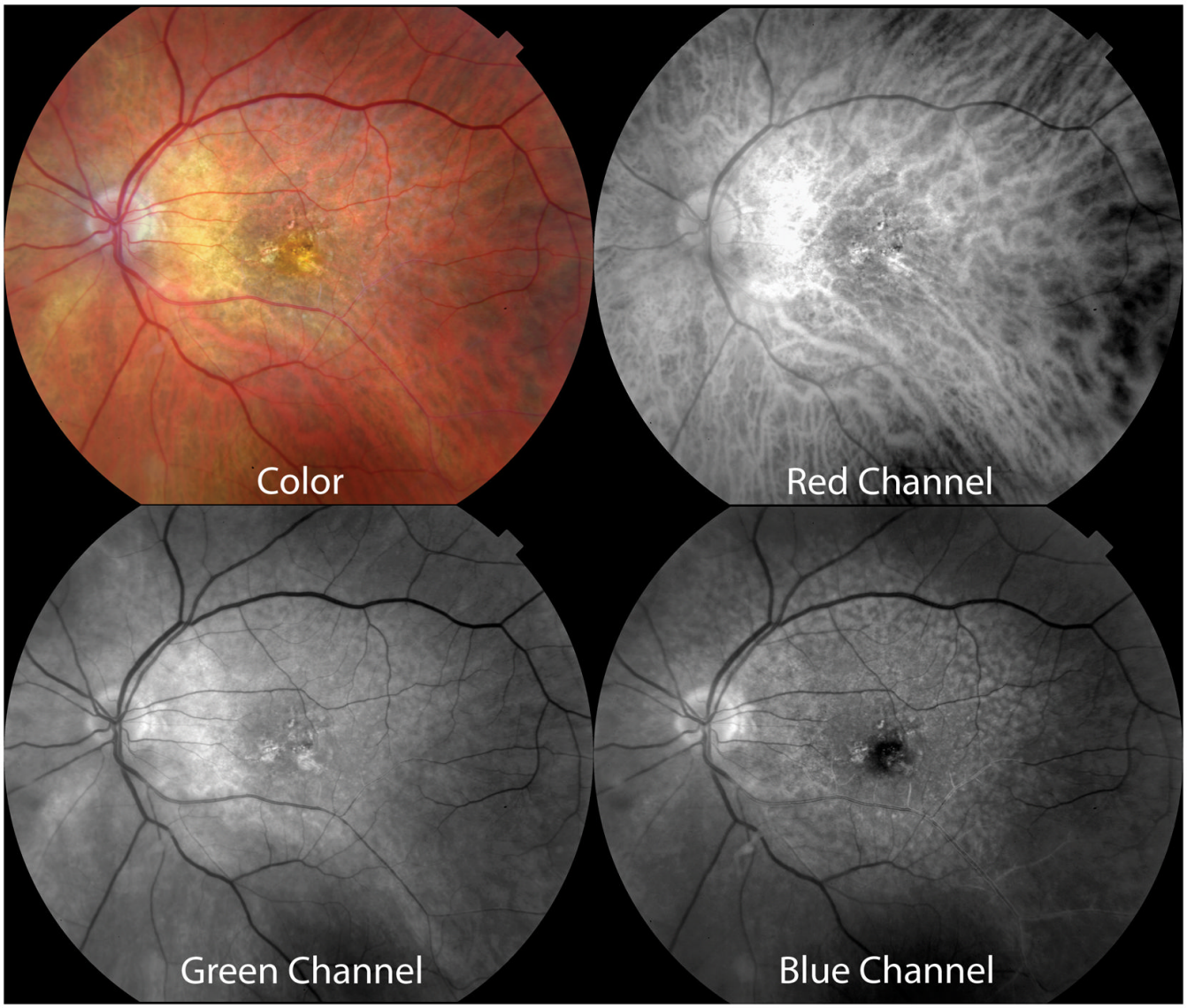

Figure 13.
Contrast between subretinal drusenoid deposits and the background. Color photograph showing subretinal drusenoid deposits and the composite color channels in the color photograph. The red channel offers little contrast between the subretinal drusenoid deposits and the underlying choroid, in part because of the high penetration of red light through the RPE and the large proportion of red light reflected by the choroidal blood vessels. The contrast between the subretinal drusenoid deposits is increased somewhat in the green channel and is most evident in the blue channel. The RPE preferentially absorbs blue light and thus offers a darker background. Note the dark central macula in the blue channel because of light absorption by the macular pigment.

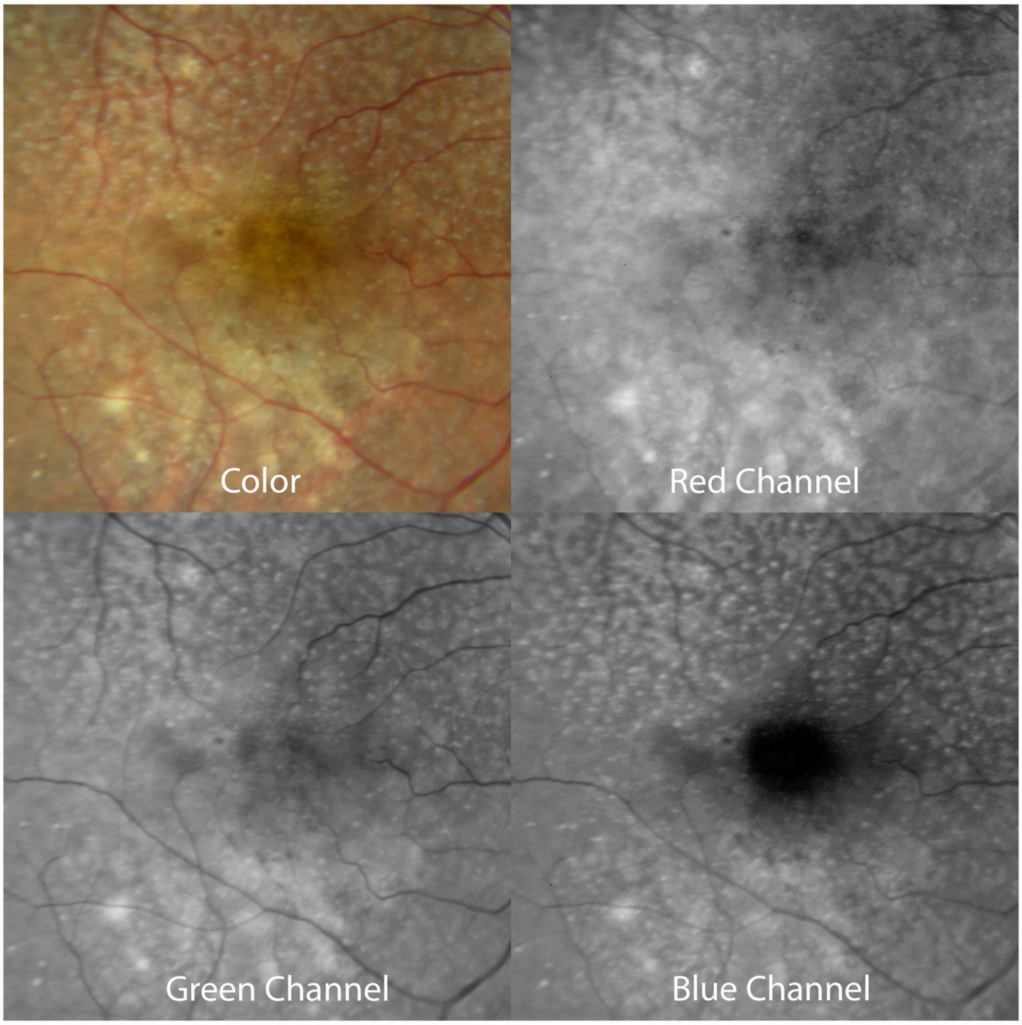

Figure 14.
Subretinal drusenoid deposits and soft drusen are distinct in different color channels. In the red channel of the color photograph, soft drusen (in superior macula) are brighter and partially reduce the visibility of the underlying choroidal vessels. In the green and blue channels, the subretinal drusenoid deposits (in inferior macula) are brighter. In the blue channel, the soft drusen are much less evident.

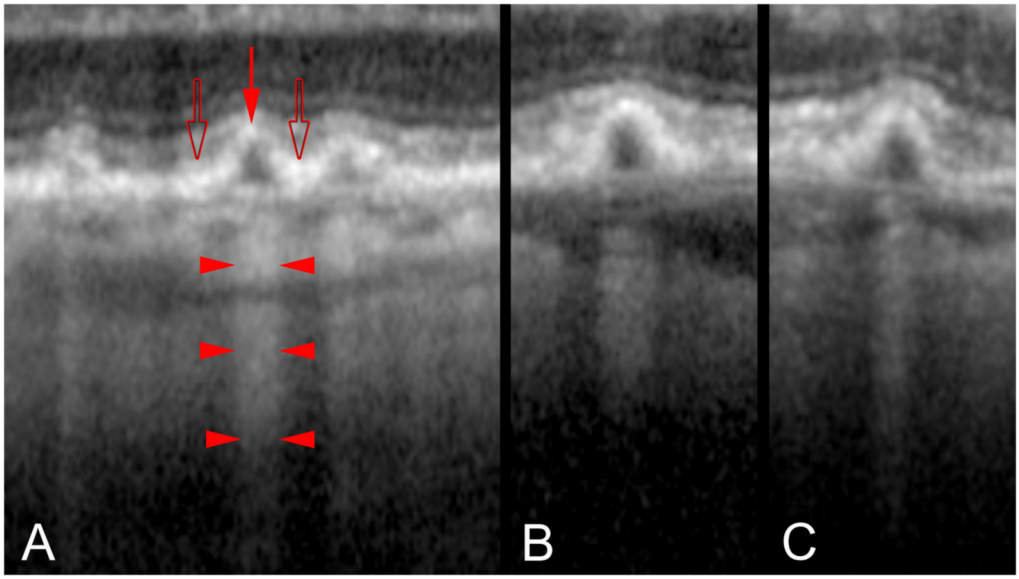

Figure 15.
Penetration of light through cuticular drusen revealed by OCT. A. Each druse shows thinning of the overlying RPE at its apex (red arrow) and RPE thickening at its base (open arrows). Penetration of light into the underlying choroid is blocked at sites adjacent to the drusen (bodies of the arrowheads) while transmission of light is increased in the center of each druse (at the points of the arrowhead). B, C. The transmission of light into the deeper layers thus varies not according to the thickness of the druse material, but by the thickness of the RPE.